International Journal of Computer Information Systems and Industrial Management Applications
ISSN 2150-7988 Volume 18 (2026) pp. 1-13

https://doi.org/10.70917/ijcisim-2026-0117
Article

Practical Exploration of Digital Twin Technology to Construct a Teaching Environment Combining Virtual and Real in Civic and Political Education

Xuefei Wang *

Nanjing Institute of Technology, Nanjing, Jiangsu, 211167, China; wxf@njit.edu.cn

Abstract: The rapid development of information technology has made digital twin technology a key driver of educational transformation. This paper combines high-performance sensors and other hardware with feature extraction algorithms and other technologies to construct an online immersive teaching system that integrates reality and virtuality, thereby achieving the digitization and virtualization of ideological and political education. The TSDF algorithm, Neural Recon algorithm, and Marching Cube algorithm are used to process spatial data at high speed, and ThingJS and GIS technology are employed to convert between virtual and real coordinates, thereby enhancing the interactive performance of the model. Research findings indicate that the model's accuracy, completeness, and average value metrics reach 0.3013 mm, 0.1718 mm, and 0.4011 mm, respectively, with iteration loss values ranging from 2.50 to 9.98, outperforming comparison models in reconstruction performance. When the model is used to assist ideological and political education, the experimental class demonstrates significantly higher ideological and political proficiency across five dimensions compared to the control class ($p < 0.01$).

Keywords: digital twin technology; virtual-physical integration; spatial data processing; ThingJS technology; ideological and political education

1. Introduction

Digital twins, as a practical application of modern technologies such as big data, cloud computing, artificial intelligence, blockchain, and virtual reality reaching their “singularity moment,” herald a new form of digital technology development, offering practical advantages in terms of technological integration, innovation, and synergistic empowerment. The strategic technological advantages they represent for China have become a cornerstone of digital transformation in social production and daily life, as well as a new growth point for innovation-driven development [1-2]. Ideological and political education, as a special social practice that guides people's ideas, political views, moral qualities, and value pursuits, will inevitably be profoundly shaped by digital twins in terms of its internal structure and existence. Based on this, prospectively exploring the potential of digital twins to empower ideological and political education is both the logical necessity of the intrinsic development of ideological and political education and the practical necessity of its digital and intelligent development [3-5].

Digital twin technology is a concept that transcends reality, based on physical models, sensor updates, and operational history datasets [6]. Digital twin technology can utilize AR, VR, and MR technologies to create immersive experiential environments based on multi-sensory stimulation, capable of simulating real-world scenarios or constructing virtual teaching environments tailored to students' learning needs [7-9]. Placing students in such an immersive learning environment enables interactive engagement between students and information technology, fostering a comprehensive educational framework that integrates behavior, thought, and belief [10-12]. Razzaq, S., et al. developed a deep classroom model for recording attendance and monitoring course content, which serves as a digital twin framework to address

the shortcomings of smart classrooms and enhance teaching efficiency [13]. Kartashova, L. A. et al. utilized digital twin technology to construct a digital prototype of an educational institution, integrating traditional teaching aids with digital resources to form a unique blended teaching format. This successfully combined educational participants in physical and virtual spaces, enabling educational processes to proceed smoothly under any circumstances [14]. Ahuja, K. et al. employed a novel computer vision-driven system to construct a digital twin model within a smart classroom, which can perceive students' classroom behavior without affecting them, thereby effectively improving teaching strategies [15]. Selim, A. et al. utilized NFC (near-field communication) protocols for user authentication and authorization in an application model combining efficient education with digital twins, significantly enhancing data transmission efficiency between real and virtual environments [16].

Therefore, in the new era of ideological and political education in higher education, it is necessary to achieve deep integration with digital twin technology, strengthen technical infrastructure to build a more comprehensive virtual reality teaching environment, and ultimately achieve the educational objectives of ideological and political theory courses in higher education.

This paper utilizes high-performance sensors to collect student learning feature data and employs high-speed data transmission and distributed cloud server storage technology to provide a data foundation for modeling teaching environments. The TSDF algorithm is used to calculate three-dimensional spatial information, while the Neural Recon algorithm's gated recurrent unit network extracts spatial data features. Combined with the Marching Cube algorithm, this further extracts surface information to achieve precise three-dimensional modeling. The ThingJS digital twin technology development platform is selected to enhance the visualization and interactivity of teaching environment modeling. Absolute coordinate systems and spatial geographic coordinate systems are converted to enhance the realism of virtual models.

2. Implementation of Virtual-Real Integration Teaching Based on Digital Twin Technology

2.1. Building an Online Immersive Teaching System Based on a Digital Twin Podium

2.1.1. Technical and Structural Analysis

Online learning feature analysis technology integrates students' attention and self-discipline (virtual) with teachers' instructional resources (real), integrates students' cognitive levels and growth processes (virtual) with teachers' personalized guidance plans (real), and interacts students' technical proficiency and comprehension abilities (virtual) with the key points and methods of classroom instruction (real). This enables precise teaching and management throughout the entire online learning process, thereby achieving the digitalization and intelligence-driven decision-making in online teaching. Virtual-physical teaching space fusion analysis technology refers to the use of big data modeling, simulation, visualization, and other technologies in cyberspace to construct a corresponding twin teaching space, thereby achieving the digitization and virtualization of all elements of the teaching space, as well as the real-time and visualization of all states of the teaching space, i.e., the construction of a digital virtual teaching space.

Therefore, the online immersive teaching system of the digital twin podium can be divided into four layers from the basic data collection layer to the top application layer: the data support layer, the modeling, calculation, and simulation layer, the functional layer, and the immersive experience layer. Each layer is closely related to the others, progressing sequentially, with each layer expanding and enriching the functions of the preceding layers. Figure 1 shows the system architecture of the online immersive teaching system based on the digital twin podium.

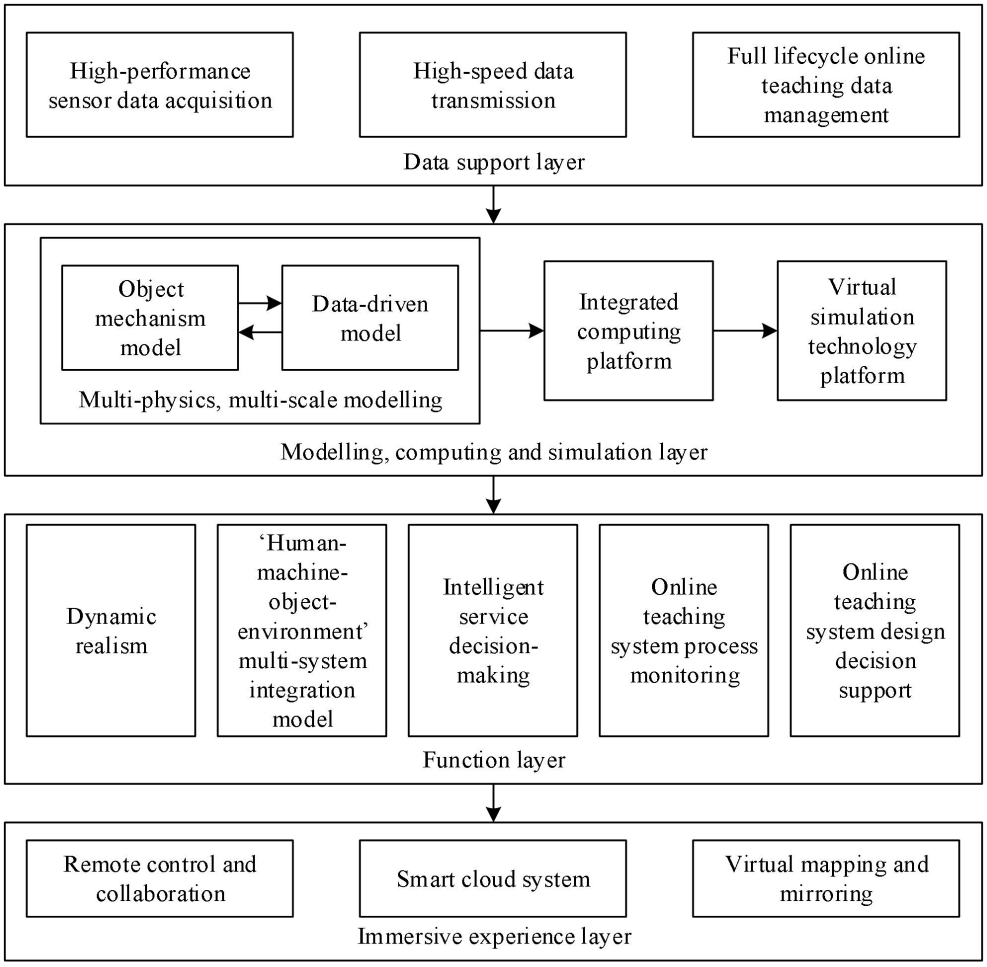

Figure 1. Online immersive teaching system based on digital twin podiums.

2.1.2. Data Support Layer

The digital twin podium relies on the interaction between real and virtual teaching spaces and IoT sensing. Therefore, the construction of an online immersive teaching system based on the digital twin podium must first start from reality and move to virtuality, using all-domain sensing devices such as cameras and smart watches to collect and capture data information in real time, thereby achieving accurate mapping between real and virtual teaching spaces. The data support layer is the key to achieving comprehensive three-dimensional sensing and serves as the foundation of the entire online immersive teaching system. It primarily consists of three components: high-performance sensor data collection, high-speed data transmission, and comprehensive lifecycle management of online teaching data.

1) The high-performance sensor data collection component utilizes wearable devices and affective computing models. For example, through students' smartwatches and other wearable devices, it collects and tracks physiological indicators and language data; through cameras installed on computers and mobile phones, it captures and collects facial expressions and body language data, supplemented by tools such as attendance rates and survey questionnaires to comprehensively and deeply collect student learning characteristic data. High-performance sensor data collection is the core technology of the data support layer. Through its intelligent sensing system, it can intelligently "read and write" the real teaching space. It serves as the 'connector' for transforming the real teaching space into a virtual teaching space in the digital twin podium, acting as the "nervous system" of the digital twin podium and the foundation for achieving its all-around intelligence.

2) The high-speed data transmission component employs high-bandwidth fiber-optic technology to transmit data such as facial expressions and body movements in real time to teachers. Additionally, the data support layer breaks through traditional auditory and visual perception by integrating sensor and IoT technologies to incorporate diverse perceptual information. As the digital twin podium is a real-time dynamic mapping of the actual online teaching space, the real-time collection, transmission, and dynamic

updating of data are of significant importance to it.

3) The full lifecycle online teaching data management component leverages distributed cloud server storage technology to ensure the storage and management of data. Its efficient storage structure and data retrieval architecture provide critical support for the storage and rapid extraction of massive, heterogeneous historical data. The massive, multi-source historical operational data also provides rich sample information for the modeling, calculation, and simulation layer, fully realizing the hyper-realistic attributes of the digital twin podium and establishing a data management system spanning the entire lifecycle.

In summary, the data support layer is essentially a data collection system based on a comprehensive, three-dimensional sensing system, enabling the comprehensive, three-dimensional, and in-depth collection of teaching data.

2.2. Model Reconstruction

After completing data collection, the next step is to build the model. The general method for multi-view 3D reconstruction involves first obtaining a depth map of the scene to reflect its depth information, then combining feature points in the image with camera poses to fuse and construct 3D structural information. When fusing structural information, implicit surface reconstruction techniques are typically employed: first, an implicit surface is constructed using truncated signed distance function (TSDF) values, and then, using deep learning techniques, spatial voxels are constructed from the TSDF to calculate the TSDF value for each voxel. In this paper, the NeuralRecon algorithm is selected for this purpose. Subsequently, the Marching Cubes algorithm is used to extract the surface.

1) TSDF Algorithm

The basic idea of the TSDF algorithm is to use a large space (i.e., volume) as a representation of a three-dimensional model and divide this space into multiple small voxels. Voxels have fixed spatial relationships, forming a three-dimensional grid composed of multiple voxels. Figure 2 shows the relationship between space volume and voxels.

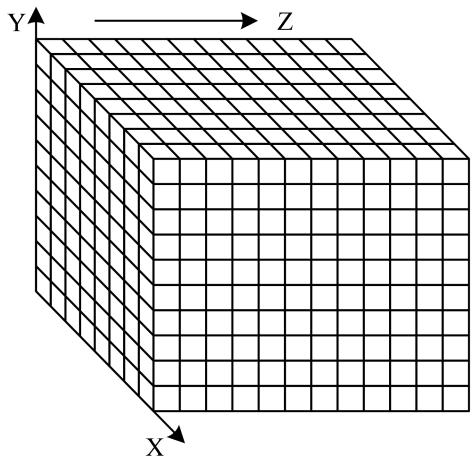

Figure 2. The relationship between vulume and voxel.

Formula (1) can be used to calculate the distance from each voxel to its nearest plane:

$$TSDF(x) = d_s - d_v \tag{1}$$

Where d_s is the depth from the plane to the camera, and d_v is the depth captured by the camera. If $TSDF(x) > 0.0$, it indicates that the voxel is in front of the real plane; if $TSDF(x) < 0.0$, it indicates that the voxel is behind the real plane; if $TSDF(x) = 0.0$, it indicates that the voxel is on the plane. By calculating the TSDF, the three-dimensional structural information of the target captured by the camera at that moment can be determined.

2) Neural Recon Algorithm

In deep learning-based 3D reconstruction algorithms, the content captured in each frame directly influences the final 3D modeling results. Therefore, to obtain the 3D structural information of the target scene, the Neural Recon algorithm adopts an incremental update approach starting from the first frame. It leverages the characteristic of 3D sparse convolutional networks, where feature layers become

increasingly dense as convolutional layers increase, to continuously update the 3D structural information (TSDF) of each frame from coarse to fine and integrate it into the global spatial volume.

During the layer-by-layer refinement process, the Neural Recon algorithm employs a gated recurrent unit (GRU) network to ensure reconstruction consistency. A GRU is a recurrent neural network that uses a gating mechanism to control information updates, enabling it to retain learned content and update it when new information is obtained. Figure 3 shows the network loop unit structure of a GRU.

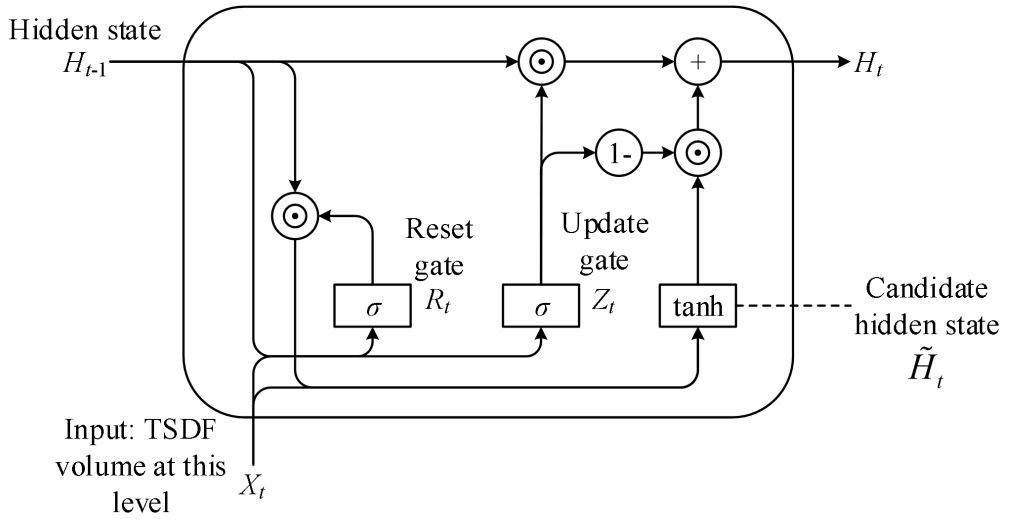

Figure 3. GRU network loop unit structure.

Compared to ordinary recurrent neural networks (RNNs), GRUs add two gate mechanisms, namely update gates and reset gates, enabling GRUs to select the information they want to focus on when constructing the hidden state of the network. The update gate is used to add important data to the candidate hidden state, while the reset gate is used to forget unimportant data. The relevant definitions are as follows:

$$R_t = \sigma\left(X_t W_{xr} + H_{t-1} W_{hr} + b_r\right) \tag{2}$$

$$Z_t = \sigma\left(X_t W_{xz} + H_{t-1} W_{hz} + b_z\right) \tag{3}$$

$$\tilde{H}_t = \tanh\left(X_t W_{xh} + (R_t \odot H_{t-1}) W_{hh} + b_h\right) \tag{4}$$

$$H_t = Z_t \odot H_{t-1} + (1 - Z_t) \odot \tilde{H} \tag{5}$$

The update gate and reset gate of the GRU can be used to determine the proportion of information from previous and current reconstructed fragments to ensure the global consistency of the reconstruction results.

3) Marching Cube Algorithm

After volume fusion, the Marching Cubes (MC) algorithm is typically used to generate the final triangular mesh model. The MC algorithm is a voxel-level reconstruction method, also known as an isosurface extraction algorithm. In three-dimensional space, an isosurface is a surface where the function value at each point is equal to a given constant V , i.e., the isosurface is a surface defined by equation (6).

$$S = \left\{(x, y, z) : F(x, y, z) = V\right\} \tag{6}$$

The MC algorithm assumes that, in a three-dimensional grid composed of cubes, the function values are uniformly distributed at the vertices of the cubes and vary linearly along the edges of the cubes. The algorithm calculates the intersection points between the isosurfaces and the edges of the cubes, and connects these points according to specific rules to obtain a sequence of polygons or triangles that approximate the isosurfaces of the model surface.

2.3. Three-Dimensional Scene Modeling and Visualization Research

2.3.1. ThingJS Digital Twin Development Technology

ThingJS is a WebGL-based 3D visualization technology designed specifically for the web platform to support the creation, rendering, and interaction of complex 3D scenes. It integrates multiple fields such as computer graphics, network technology, data visualization, and human-computer interaction. ThingJS leverages WebGL technology at its core, enabling high-performance 3D graphics rendering in web browsers without requiring any plugins. By adopting fundamental principles and techniques from computer graphics, such as lighting models, texture mapping, shadow calculation, and geometric transformations, ThingJS can create realistic 3D scenes and animations.

ThingJS supports interaction with backend services by importing various data formats (such as GeoJSON, 3DTiles, fbx, etc.). This data-driven approach allows ThingJS to be used for displaying and analyzing large amounts of geospatial data, city models, real-time data, etc., which is of great significance for fields such as GIS, smart cities, and digital twins. ThingJS provides rich interactive features, such as view control, object selection, and time response, demonstrating its powerful 3D visualization and interaction capabilities in digital twin development.

This study utilized the ThingJS development platform to construct a 3D scene model for a digital twin podium, integrate the model with GIS, and develop functional modules for the digital twin podium visualization monitoring system, including 3D scene navigation, real-time dynamic monitoring, and anomaly alerts. Finally, the system functionality was validated through the ThingJS platform. The following are several key advantages of selecting ThingJS as the digital twin development platform:

1) Highly realistic 3D visualization: ThingJS supports highly realistic 3D scene rendering based on WebGL, accurately reflecting the state of the physical world. The 3D scene model data volume is significantly smaller compared to oblique photography models, enabling low-latency dynamic interaction and a more intuitive visual experience.

2) Real-time data integration: ThingJS supports real-time data integration and display, enabling the digital twin model to reflect the real-time state of the physical world. Using WebSocket real-time data streaming technology, the model's state can be updated in real time, such as temperature changes or student learning status.

3) Interactivity: ThingJS offers rich interactive features, allowing users to control the 3D scene perspective, data queries, and dynamic interactions with simple operations, enabling more intuitive access to the model's current state and operational data.

4) Cross-platform compatibility: Based on WebGL technology, ThingJS has excellent cross-platform compatibility and can run on various devices and most mainstream browsers currently available.

2.3.2. Model Coordinate Transformation Methods

The most effective method for integrating models with GIS is through coordinate transformation. The coordinates of the constructed model are based on a relative coordinate system centered at the model's origin, with coordinate values for elements such as seats, aisles, and cameras defined relative to this origin. In the physical world, however, a unified absolute coordinate system is used, typically the WGS84 coordinate system, for spatial geographic positioning. Therefore, it is necessary to convert from the relative coordinate system to the absolute coordinate system. First, convert the model's relative coordinate system to the absolute coordinate system, and then convert the spatial rectangular coordinate system to the spatial geographic coordinate system.

1) Conversion from relative coordinate system to absolute coordinate system

Convert the constructed model coordinate system to the absolute coordinate system based on the model origin coordinates, and then convert the converted absolute coordinate system to the spatial geographic WGS84 coordinate system.

$$\begin{bmatrix} x \\ y \\ z \end{bmatrix} = \begin{bmatrix} a \\ b \\ c \end{bmatrix} + M_{n-1} \begin{bmatrix} x \\ y \\ z \end{bmatrix}_{n-1} \tag{7}$$

$$M = \begin{bmatrix} \cos\lambda & \sin\lambda & 0 \\ -\sin\lambda & \cos\lambda & 0 \\ 0 & 0 & 1 \end{bmatrix} \begin{bmatrix} \cos\beta & 0 & -\sin\beta \\ 0 & 1 & 0 \\ \sin\beta & 0 & \cos\beta \end{bmatrix} \begin{bmatrix} 1 & 0 & 0 \\ 0 & \cos\alpha & \sin\alpha \\ 0 & -\sin\alpha & \cos\alpha \end{bmatrix} \tag{8}$$

In the equation, x, y, z are the coordinates of the model in the Cartesian coordinate system, α, β, λ are the rotation angles around the x, y, z axes during coordinate transformation, and a, b, c are the initial Cartesian coordinates during coordinate transformation.

2) Conversion from spatial Cartesian coordinate system to spatial geographic coordinate system

The most commonly used absolute coordinate system is the coordinate system (λ, φ, h) under the WGS84 Earth model. First, calculate the normalized radius N:

$$N = \frac{a}{\sqrt{(1-e^2)\sin^2\varphi}} \tag{9}$$

In the formula, N is the distance from the surface of the Earth ellipsoid at a given latitude to its center of mass, a is the Earth's equatorial radius, and e is the first eccentricity. The formula for calculating the relative coordinate system is:

$$\begin{bmatrix} X \\ Y \\ Z \end{bmatrix} = \begin{bmatrix} (N+h)\cos\varphi\cos\lambda \\ (N+h)\cos\varphi\sin\lambda \\ ((1-e^2)N+h)\sin\varphi \end{bmatrix} \tag{10}$$

The coordinates of a point in the spatial coordinate system are converted to coordinates in the absolute coordinate system with the Earth's center of mass as the origin using the above conversion formula.

The formula for calculating the geodetic longitude λ is as follows:

$$\lambda = \tan^{-1}\left(\frac{Y}{X}\right) \tag{11}$$

The calculation of latitude φ and altitude h is relatively complex, as they are interdependent. Therefore, an iterative method is used for calculation. Assuming an initial value for latitude φ:

$$\varphi = \tan^{-1}\frac{Z}{\sqrt{X^2+Y^2}} \tag{12}$$

Calculate a new height h using the initial latitude φ:

$$N = \frac{a}{\sqrt{(1-e^2)\sin^2\varphi}} \tag{13}$$

$$h = \frac{\sqrt{X^2+Y^2}}{\cos\varphi} - N \tag{14}$$

Through iterative calculations until the latitude φ and height h converge. Based on spatial coordinate system conversion formulas, complementary requirements can be achieved in different coordinate system scenarios. This allows the constructed virtual model to be assigned spatial geographic location information, enabling precise positioning in the corresponding location in a 3D GIS scene when loading the model, thereby achieving integration between the virtual model and GIS.

3. Model Performance Verification and Application Analysis

3.1. Relationship between Depth Distance and Root Mean Square Error

Figure 4 shows the root mean square error (RMSE) of depth values corresponding to different depth ranges of the sensor during model reconstruction. When the depth does not exceed 3000 mm, the root mean square error of the depth values is 20 mm or less; however, when the depth exceeds 3000 mm, the error can reach approximately 49 mm, at which point the error becomes significant. Therefore, to ensure modeling accuracy, when using hardware sensors to collect and capture data sets, it is advisable to keep the distance between the sensors and the students below 3000 mm.

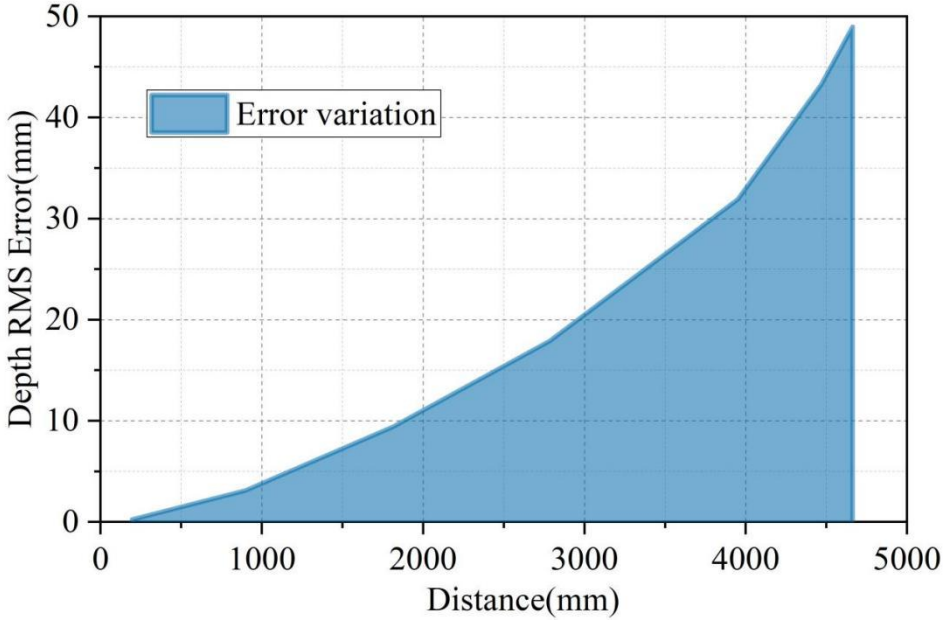

Figure 4. Relationship between depth distance and root mean square error.

3.2. Dataset Experiments and Analysis

3.2.1. DTU Dataset Experimental Results and Analysis

After constructing the digital twin podium model using the method described above, a unified configuration was adopted to test the model's performance on the DTU dataset and the Tanks and Temples dataset. This section first conducted tests on the DTU dataset, evaluating the model constructed in this paper using three metrics: accuracy (Acc.), completeness (Comp.), and overall average (Overall). The model was then compared with traditional geometry-based methods and existing deep learning-based models (lower values indicate higher model precision).

Table 1 shows the comparison results of evaluation metrics for different models on the DTU dataset. As shown in Table 1, in terms of accuracy, the model proposed in this paper performed the best, achieving an accuracy of 0.3013 mm. In terms of completeness, the model proposed in this paper led with a score of 0.1718 mm, representing a 67.76% improvement compared to the baseline model (0.5329 mm). This indicates that, compared to other methods, the proposed model has a significant advantage in terms of the completeness of the reconstructed teaching environment, enabling the recovery of a more complete 3D model. Additionally, in terms of the mean metric, the proposed model also ranks first, achieving a score of 0.4011 mm, which is 0.0568 mm lower than the baseline model, representing an improvement rate of 12.40%.

Table 1. Comparison of evaluation metrics on the DTU dataset.

Method	Acc.(mm)	Comp.(mm)	Overall(mm)
Gipuma	0.4907	0.7705	0.6801
COLMAP	0.6072	0.5611	0.6346
R-MVSNet	0.5923	0.3563	0.5247

PatchmatchNet	0.6345	0.1745	0.4541
EPP-MVSNet	0.6204	0.1938	0.4573
CVP-MVSNet	0.5032	0.3032	0.4535
MVSNet	0.6037	0.4241	0.5648
Baseline (CasMVSNet)	0.5329	0.2824	0.4579
Ours	0.3013	0.1718	0.4011

Figure 5 shows the changes in the loss function during the training process of the model in this paper on the DTU dataset. It can be seen that the value of the loss function decreases rapidly in the first 14k iterations, from over 9.98 to around 5.01. From 15k to 90k iterations, it continues to decrease steadily, with the rate of decrease gradually slowing down. The value of the loss function decreases from 5.01 to around 2.62. In subsequent iterations, the loss function value stabilizes around 2.50. The model exhibits a small and highly stable loss function value during training on the DTU dataset.

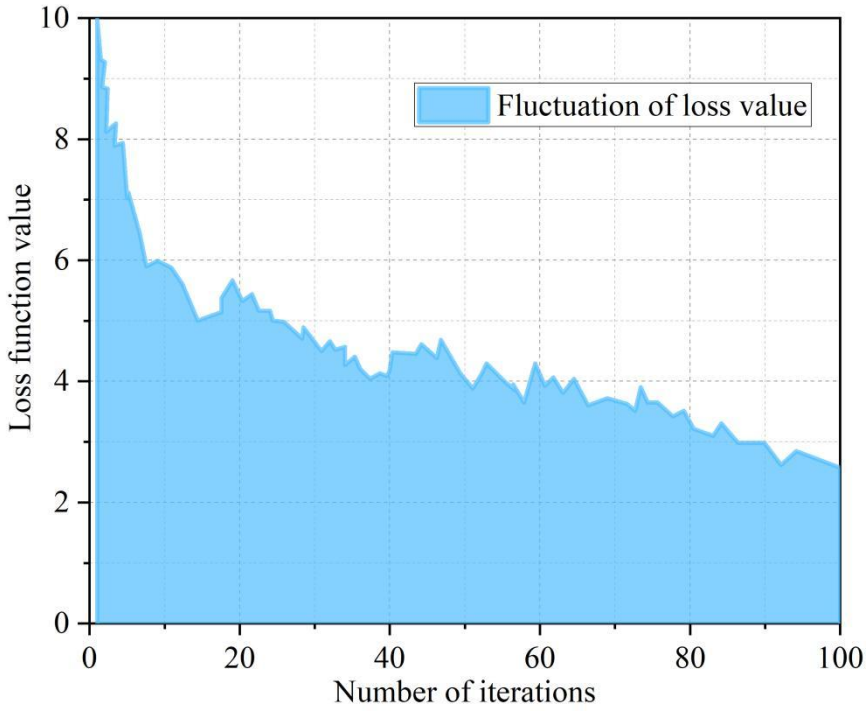

Figure 5. Loss function variation of the model in this paper on DTU.

3.2.2. Experimental Results and Analysis of the Tanks and Temples Dataset

In the previous section, we compared the quantitative and qualitative experimental results of the DTU dataset. It is important to note that the model presented in this paper was trained on the DTU dataset, which was collected under strictly controlled laboratory conditions. This factor may have contributed to the model's performance to some extent. To more comprehensively evaluate the model's generalization ability, this section will test it on the Tanks and Temples dataset and compare the results with other depth estimation methods. Table 2 presents the detailed comparison results. In the comparison of 9 metrics, the metrics of the model proposed in this paper are 69.45, 87.34, 69.62, 67.87, 73.82, 71.74, 74.72, 69.55, and 70.27, respectively, all of which are higher than the other 6 comparison models. This proves that the model proposed in this paper has better generalization performance in scene reconstruction in large-scale educational environments.

Table 2. Comparison of evaluation indicators in Tanks and Temples.

Method	Mean	Family	Francis	Horse	L.H.	M60	Panther	P.G.	Train
COMLAP	43.43	53.27	25.72	30.31	60.61	48.46	52.21	50.31	45.91
CasMVSNet	58.21	79.12	61.01	50.01	60.06	59.63	59.32	60.02	53.11
Vis-MVSNet	61.33	80.55	63.59	50.83	67.37	65.71	62.53	62.32	55.03
PatchmatchNet	54.72	69.87	56.42	46.96	59.18	56.43	54.78	56.05	54.77
R-MVSNet	51.02	75.26	57.97	47.13	48.24	50.32	50.95	56.71	41.21
AA-RMVSNet	62.38	80.13	62.91	55.27	50.22	67.12	62.75	62.69	58.86
Ours	**69.45**	**87.34**	**69.62**	**67.87**	**73.82**	**71.74**	**74.72**	**69.55**	**70.27**

3.3. Comparative Experiments and Analysis of Results

A virtual-reality integrated teaching model for ideological and political education, based on digital twin technology, was applied to first-year students majoring in Marxism at Y University. A one-year controlled experiment was conducted. Class A was selected as the experimental class, where the model was used to assist ideological and political education; Class B was selected as the control class, where traditional teaching methods were used. Both classes had 40 students, and their average entrance examination scores were consistent. There were no other variables besides the teaching methods. To better reveal the commonalities and differences in the emotional attitudes and values of students in the experimental and control classes, the survey results were first subjected to statistical analysis, followed by a differential analysis of the emotional attitudes and values of students in the experimental and control classes using SPSS 26.0.

3.3.1. Comparative Analysis of the Ideological and Political Emotional Dimension

To understand changes in students' ideological and political emotions, we primarily examine three secondary dimensions: students' understanding of ideological and political education, their interest in learning ideological and political education, and their experiences in learning ideological and political education. Among these, understanding of ideological and political education primarily encompasses students' perceptions of the subject, its knowledge, thinking, and ideology; interest in learning ideological and political education focuses on students' interest in numerical relationships and spatial structures in real life, their willingness to participate in ideological and political education classroom activities, and their willingness to apply ideological and political education knowledge to solve problems; and learning experiences primarily involve students' sense of joy and accomplishment in learning ideological and political education. Figure 6 presents the average statistical scores for each indicator under the ideological and political education emotional dimension. After the experiment, the average scores for the three dimensions of ideological and political education recognition, interest, and experience in the experimental class were 4.582, 4.773, and 4.695 points, respectively, which were 0.963, 1.209, and 0.873 points higher than those of the control class. Applying the model proposed in this paper to assist ideological and political education can enhance students' emotional engagement in learning ideological and political education courses.

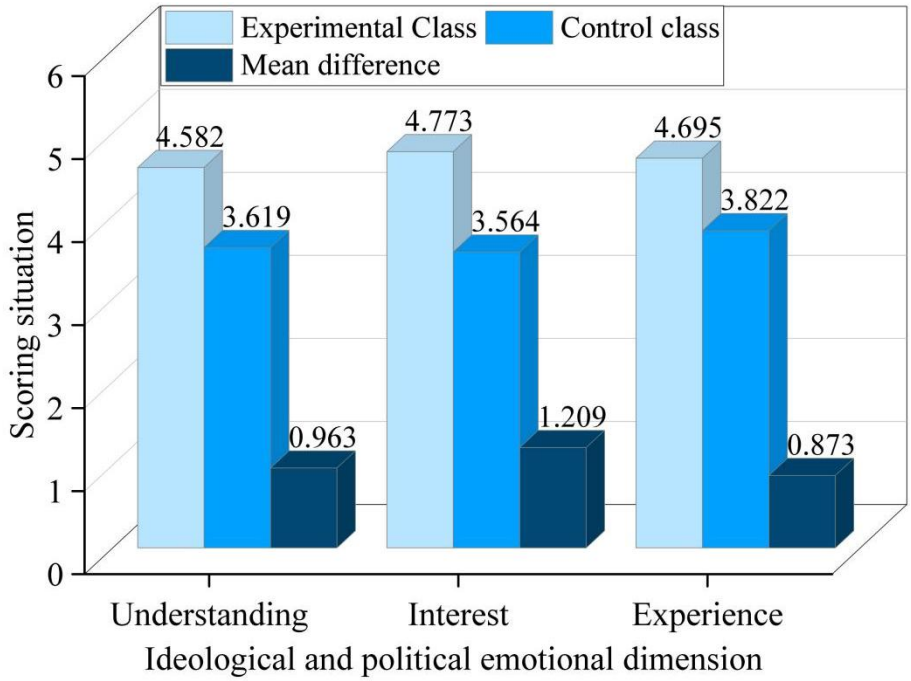

Figure 6. Average scores of each index under the emotional dimension.

3.3.2. Comparative Analysis of Ideological and Political Attitude Dimensions

The attitude toward ideological and political education learning comprises two dimensions: learning motivation and learning beliefs. Learning motivation includes factors such as curiosity and a desire for knowledge, while learning beliefs encompass factors such as confidence in learning ideological and political education and a firm commitment to ideological and political ideals. Figure 7 shows the average scores for each indicator under the ideological and political education attitude dimension for the two classes. The average score for learning motivation in the experimental class was 4.826 points, which was 1.807 points higher than the 3.019 points in the control class; the average score for learning beliefs was 4.725 points, which was 1.449 points higher than the 3.276 points in the control class. Based on the comparison of average scores, using the model proposed in this paper to assist teaching can also help students adopt a proper attitude toward ideological and political education courses.

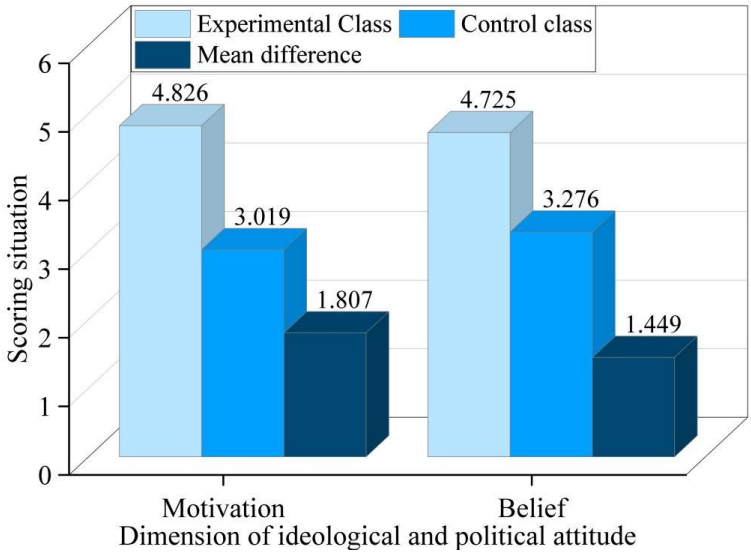

Figure 7. Average scores of each indicator under the attitude dimension.

3.3.3. Analysis of Differences in Students' Emotional Attitudes

Since the aforementioned analyses were all simple statistical analyses, it was impossible to determine whether there were significant differences between the experimental class and the control class. Therefore, class was used as the grouping variable, and ideological and political awareness, ideological and political interest, ideological and political experience, ideological and political learning motivation, and ideological and political learning beliefs were used as test variables. SPSS 26.0 was used to perform a difference analysis.

Table 3 presents the results of the differential analysis of students' emotional attitudes. The significance levels for the five dimensions were 0.001, 0.004, 0.004, 0.001, and 0.001, respectively, all of which were less than 0.01, indicating that there were significant differences between the experimental and control classes in all five dimensions. The use of a virtual-physical integrated teaching model for ideological and political education, constructed based on digital twin technology, can significantly enhance students' ideological and political learning outcomes.

Table 3. Analysis of the Differences in Students' Emotional Attitudes.

Ideological and political dimension	Average value equivalence t-test		Difference of 95% confidence interval	
	Average value difference	Significance level sig. (Double tail)	Lower limit	Upper limit
Understanding	0.41585	0.001	0.10238	0.87521
Interest	0.42543	0.004	0.12406	0.64577
Experience	0.45302	0.004	0.16348	0.75400
Motivation	0.40051	0.001	0.24967	0.82516
Belief	0.32724	0.001	0.27831	0.29845

4. Conclusion

This paper utilizes digital twin development technology and data collection devices to construct an online immersive ideological and political education system that integrates virtual and real elements, and evaluates its performance and application advantages. The model achieves an accuracy of 0.3013 mm, with completion rates and average values improved by 67.76% and 12.40% respectively compared to the baseline model. The loss value does not exceed 9.98, and the iteration process is relatively stable. In a comparison of nine metrics across a large dataset, the model demonstrated superior reconstruction performance. The experimental class outperformed the control class by 0.963, 1.209, and 0.873 points across three dimensions of ideological and political emotions, and by 1.807 and 1.449 points across two dimensions of ideological and political attitudes. The experimental class was significantly superior to the control class at the 0.01 level. In the future, the impact of data collection depth on the root mean square error can be further reduced to improve modeling accuracy.

References

1. Tong, W., Wang, Y., Su, Q., & Hu, Z. (2022). Digital twin campus with a novel double-layer collaborative filtering recommendation algorithm framework. Education and Information Technologies, 27(8), 11901-11917.
2. Arantes, J. (2024). Digital twins and the terminology of “personalization” or “personalized learning” in educational policy: A discussion paper. Policy Futures in Education, 22(4), 524-543.
3. Luo, S. (2022). Construction of situational teaching mode in ideological and political classroom based on digital twin technology. Computers and Electrical Engineering, 101, 108104.
4. Ye, H. (2021, June). A review on the application of virtual reality technology in ideological and political teaching. In 2021 2nd International Conference on Artificial Intelligence and Education (ICAIE) (pp. 712-715). IEEE.
5. Wang, J. (2022). Logical Innovation of Metaverse Empowerment Ideological and Political Education: Reconstruction Based on People, Things and Scenes. Academic Journal of Humanities & Social Sciences, 5(18), 92-99.
6. Han, X., Yu, H., You, W., Huang, C., Tan, B., Zhou, X., & Xiong, N. N. (2022). Intelligent campus system design based on digital twin. Electronics, 11(21), 3437.

7. Habarurema, J. B., Di Fuccio, R., & Limone, P. (2025). Enhancing e-learning with a digital twin for innovative learning. The International Journal of Information and Learning Technology.
8. Ezeoguine, P. E., & Kasumu, R. Y. (2024). Undergraduate Students' Perception of Digital Twins Technology in Education: Uses and Challenges. Int. J. Educ. Eval., 10(2), 381-396.
9. Chamorro-Atalaya, O., Flores-Velásquez, C. H., Flores-Cáceres, R., Arévalo-Tuesta, J. A., Zevallos-Castañeda, M., Tomás-Quispe, G., ... & Alarcón-Anco, R. (2024). Use of Digital Twin Technology in the Teaching-Learning Process, in the field of University Education: A Bibliometric Review. International Journal of Learning, Teaching and Educational Research, 23(2), 313-329.
10. Fiore, M., Gattullo, M., & Mongiello, M. (2024, March). First steps in constructing an AI-powered digital twin teacher: harnessing large language models in a metaverse classroom. In 2024 IEEE Conference on Virtual Reality and 3D User Interfaces Abstracts and Workshops (VRW) (pp. 939-940). IEEE.
11. Damaševičius, R., & Zailskaitė-Jakštė, L. (2024). Digital twin technology: Necessity of the future in education and beyond. Automated Secure Computing for Next-Generation Systems, 1-22.
12. She, M., Xiao, M., & Zhao, Y. (2023). Technological implication of the digital twin approach on the intelligent education system. International journal of humanoid robotics, 20(02n03), 2250005.
13. Razzaq, S., Shah, B., Iqbal, F., Ilyas, M., Maqbool, F., & Rocha, A. (2023). DeepClassRooms: a deep learning based digital twin framework for on-campus class rooms. Neural Computing and Applications, 1-10.
14. Kartashova, L. A., Gurzhii, A. M., Zaichuk, V. O., Sorochan, T. M., & Zhuravlev, F. M. (2020). Digital twin of an educational institution: an innovative concept of blended learning. In Proceedings of the symposium on advances in educational technology, aet.
15. Ahuja, K., Shah, D., Pareddy, S., Xhakaj, F., Ogan, A., Agarwal, Y., & Harrison, C. (2021, May). Classroom digital twins with instrumentation-free gaze tracking. In Proceedings of the 2021 chi conference on human factors in computing systems (pp. 1-9).
16. Selim, A., Ali, I., Saracevic, M., & Ristevski, B. (2024). Application of the digital twin model in higher education. Multimedia Tools and Applications, 1-18.